Hindawi
Mathematical Problems in Engineering
Volume 2019, Article ID 2535980, 11 pages
https://doi.org/10.1155/2019/2535980

Research Article

Thermal Diffusion Effects in a Tunnel with a Cylindrical Lining and Soil System under Explosive Loading

Minjie Wen,[1] Jinming Xu ,[1] and Houren Xiong [2]

[1]*Department of Civil Engineering, Shanghai University, Shanghai 200444, China*
[2]*College of Civil Engineering and Architecture, Jiaxing University, Jiaxing, Zhejiang 314001, China*

Correspondence should be addressed to Jinming Xu; xjming@163.com

Received 19 December 2018; Accepted 5 March 2019; Published 20 March 2019

Academic Editor: Francesco Marotti de Sciarra

An analytical method is employed to study the thermoelastic dynamic response of deep-buried circular tunnel lining-soil system under explosion load, considering thermal diffusion effects. The soil and lining are analyzed as homogeneous elastic media. Based on the generalized thermal diffusion theory and the classical thermal elasticity theory, the thermoelastic dynamic response of a soil-lining system in the event of an explosion is solved using the Laplace transform and Helmholtz decomposition. By using continuity boundary conditions, the corresponding numerical solution is obtained through an inverse Laplace transform. The calculated results are compared to those without the lining and without consideration for the diffusion effect. The effects are analyzed under thermal, mechanical, and chemical coupling of the lining and soil properties, and their geometric parameters on the temperature gradient, displacement, stress, and chemical potential of the system. It provides significant guidance for theoretical calculations and antiexplosion design of the lining tunnel.

1. Introduction

Underground lining structures, such as subway tunnels, heat distribution pipelines, petroleum pipelines, and gas pipelines can generate high temperatures and pressures when subjected to endogenous explosive loads, which often cause extensive damage to the lining structure and the surrounding geomaterials, such as crushing, cracking, and deformation. In previous research, the problem of analyzing the underground lining structure under explosive loading was equivalent to the endogenous force load, which ignored the impact of high temperature caused by explosion [1–5]. At the moment of the explosion, the temperature and stress in the soil and lining interact with each other. Therefore, considering the thermal coupling effect, it is of great engineering significance to study the dynamic response of the lining structure and soil under loads from explosions.

At the present time, there are relatively few studies on the thermoelastic dynamic response of soil and underground structures that include coupling between thermal effects and stresses. In the 1960s, Nowacki et al. obtained a thermoelastic diffusion behavioral model based on a thermoelastic coupling model [6–9]. However, in this theory, the heat propagation rate was considered to be infinite. In order to avoid this problem, many scholars extended that analysis to introduce the thermal relaxation time to obtain a generalized thermoelastic theory [10–12]. Zhao Weitao et al. [13] used G-L generalized thermoelastic theory with two thermal relaxation times, to study the thermoelastic response of solid spheres that were subjected to a suddenly applied load with a homogeneous distribution on the spheres' external surfaces and analyzed the effects of the thermal relaxation time and coupling coefficient on their displacement and temperature distribution. Wang et al. [14] employed a Fourier series expansion method to study the one-dimensional thermoelastic problem. Chandrasekharaiah et al. [15] studied the thermoelastic response problem of a half-space elastic body under thermal shock and derived the analytical expressions for the temperature gradient, displacements, and stresses, using the Laplace transform and inverse transform. Based on the generalized thermoelastic theory, Dhaliwal and Sherief [16] obtained the thermoelastic dynamic response of a half-space elastic body seeing a point heat source load and

analyzed the temperature distribution in the depth direction. Sherief et al. [17] obtained the thermoelastic response of an infinite elastic body around a spherical cavity using a Laplace transform approach and found the corresponding numerical solution by means of the Laplace inverse transformation. It has been modified by Sherief based on the Nowacki thermoelastic diffusion theory. Singh et al. [18] studied the propagation characteristics of thermoelastic waves by introducing a displacement potential function and analyzed the reflections of P waves and SV waves on the free surfaces of an elastic body. Aouadi [19] studied the thermoelastic diffusion problem of spherical cavities in infinite elastic bodies and obtained the thermoelastic response of elastomers under thermal, mechanical, and chemical coupling. Zheng Rongyue et al. [20] considered the thermal diffusion effect to study the dynamic response of an infinite soil mass with a circular tunnel considering thermoelastic coupling and analyzed the temperature distribution, stress, displacement, and chemical potential. Liu Ganbin et al. [21] and Lu Zheng et al. [22] obtained the dynamic response of porous elastic media under the thermo-hydro-mechanical coupling effect, based on the thermoelastic theory and the generalized thermoelastic theory. The integral form and numerical solutions were obtained by using the Fourier transform and inverse Fourier transform, respectively. Sherief et al. [23, 24] obtained the fractional heat conduction equation according to the definitions by Caputo and Riemann-Liouville, and Youssef [25] obtained the fractional heat conduction equation by means of fractional Taylor expansion method. This latter method was successfully employed by many scholars to analyze problems such as low temperature, thermal shock, and responses to explosions [26–31]. However, these results did not take into account the combination of shock waves and high temperatures caused by explosions and ignored the effect of linings. This paper considers the interaction between linings and soils. The thermoelastic dynamic response of the deeply buried circular tunnel lining-soil system under explosion loads is studied by employing more realistic force load and thermal shock load formulas to simulate an explosion's effects. Based on generalized thermal diffusion theory and the classical thermoelastic theory, the thermoelastic dynamic response of the soil-lining system under the action of an explosion is obtained. Using continuity boundary conditions, the corresponding numerical solution can be obtained by a Laplace inverse transformation. The effects of lining and soil properties and geometric parameters on the temperature gradients, displacements, stresses, and chemical potential of the system are analyzed under thermal, mechanical, and chemical coupling. Also, compared with the existing calculated results, the correctness of calculated results is verified, which provides guiding significance for the theoretical calculation and antiexplosion design of the lining tunnel.

2. Mathematical Model and Basic Assumptions

The system diagram which the calculations are based on is shown in Figure 1. A cylindrical tunnel lining is deeply buried in the infinite soil body. The inner and outer diameters of the lining are R_1 and R_2, respectively, and the lining

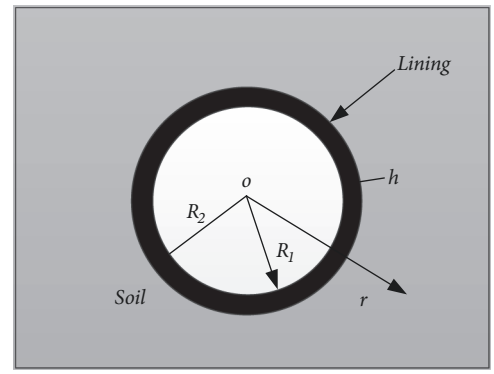

Figure 1: The interaction model between lining and soil.

wall thickness is $h = R_2\text{-}R_1$. The inner wall of the lining structure is subjected to a radial uniformly distributed load from an explosion $T(t)$. According to prior work [32], an explosion's load is a combination of force and heat source loads. When an explosion occurs in the center of the tunnel, the explosion's shock wave is assumed to be emitted from the tunnel's center. After encountering the lining's inner wall an explosion's shock waves will be reflected many times, and the maximum pressure shows the tendency towards attenuation of vibrations. Thus, the simplified force source load pattern in Figure 2(a) is used as a high-pressure load source simulating the inner wall of the lining. Due to the high temperatures seen while subjected to high pressure shock waves and the studies showing that the temperatures decrease exponentially, the simplified heat source load pattern in Figure 2(b) is used to simulate high temperatures. Assuming that the surrounding soil and lining are homogeneous elastic media, the lining-soil system undergoes small deformations only. If the lining and tunnel are infinitely long, the problem can be regarded as a plane strain model for analysis. The interface between the lining and the soil is assumed to be bonded (without relative slip), which satisfies the continuity boundary condition.

For the axisymmetric problem, regardless of physical force, the kinematic equation, heat conduction equation, and thermal diffusion equation of soil are all expressed by

$$\left(\lambda^{S} + 2\mu^{S}\right)\frac{\partial e^{S}}{\partial r} - \beta_1\frac{\partial \theta^{S}}{\partial r} - \beta_2\frac{\partial M}{\partial r} = \rho^{S}\frac{\partial^2 u_r^{S}}{\partial t^2} \quad (1)$$

$$\left(\frac{\partial}{\partial t} + \tau_0\frac{\partial^2}{\partial t^2}\right)\left(\rho^{S}c_s\theta^{S} + \beta_1 T_0 e^{S} + c_1 T_0 M\right) = \kappa^{S}\nabla^2\theta^{S} \quad (2)$$

$$D\beta_2\nabla^2 e^{S} + Dc_1\nabla^2\theta^{S} + \frac{\partial M}{\partial t} + \tau\frac{\partial^2 M}{\partial t^2} = Db\nabla^2 M \quad (3)$$

where $e^{S} = \partial(ru_r^{S})/r\partial r$ denotes the volumetric strain, $\theta^{S} = T - T_0$ denotes the temperature gradient, and T, T_0 denote the absolute temperature and the initial temperature, respectively, $|(T - T_0)/T_0| \ll 1$, $\beta_1 = (3\lambda^{S} + 2\mu^{S})\alpha_t$ denote the thermoelastic modulus, α_t denotes the linear thermal expansion coefficient, $\lambda^{S} = 2\nu^{S}\mu^{S}/(1 - 2\nu^{S})$ and $\mu^{S} = G^{S}$ are the Lame constants, ν^{S} denotes the Poisson's ratio of the soil, and G^{S} denotes the shear modulus. In

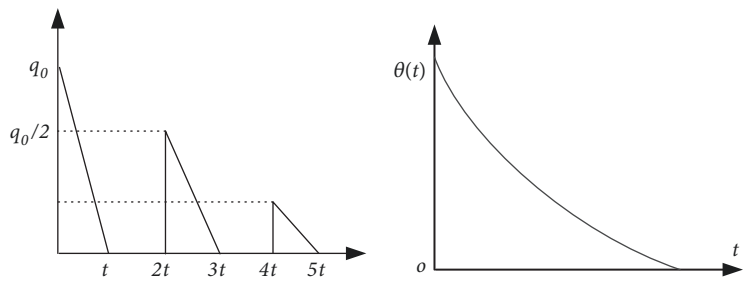

(a) Force source load (b) Heat source load

Figure 2: Simplified explosion load pattern.

$\beta_2 = (3\lambda^S + 2\mu^S)\alpha_c$, α_c denotes the expansion coefficient of linear thermal diffusion, M denotes the intensity of diffusion flow, ρ^S denotes the density of the soil, and u_r^S denotes the radial displacement. Parameters τ_0, τ denote the thermal relaxation time and the diffusion relaxation time, respectively, c_s denotes the specific heat of the soil, c_1, b denote the thermal diffusion influence coefficients, κ^S denotes the heat transfer coefficient, D denotes the diffusion coefficient, and ∇^2 denotes a differential operator.

The stress-strain constitutive relationship of the soil with consideration of temperature effects is defined by

$$\sigma_r^S = 2\mu^S \frac{\partial u_r^S}{\partial r} + \lambda^S e^S - \beta_1 \theta^S - \beta_2 M \tag{4}$$

$$\sigma_\theta^S = 2\mu^S \frac{u_r^S}{r} + \lambda^S e^S - \beta_1 \theta^S - \beta_2 M \tag{5}$$

$$P = -\beta_2 e^S + bM - c_1 \theta^S \tag{6}$$

where P denotes the chemical potential. Variables $\sigma_r^S, \sigma_\theta^S$ denote the radial and hoop stresses of the soil.

Considering the explosion load as the combination of a force source and a heat source load, the Laplace transform form of the force load $q(t)$ and heat source $\theta(t)$ is as follows:

$$\begin{aligned}\overline{q}(s) = {} & \frac{q_0}{s} + \frac{q_0}{\bar{t}s^2}\left(e^{-s\bar{t}} - 1\right) \\ & + \frac{q_0}{2\bar{t}}\left[\frac{e^{-3s\bar{t}}}{s^2} + \left(\frac{5\bar{t}}{s} - \frac{1}{s^2}\right)e^{-2s\bar{t}}\right] \\ & + \frac{q_0}{4\bar{t}}\left[\frac{e^{-5s\bar{t}}}{s^2} + \left(\frac{9\bar{t}}{s} - \frac{1}{s^2}\right)e^{-4s\bar{t}}\right]\end{aligned} \tag{7}$$

where $\bar{t}$ denotes the dimensionless loading time. The Laplace transform of $\theta(t)$ is

$$\overline{\theta}(s) = \frac{\theta_0}{s + 0.5} \tag{8}$$

where q_0, θ_0 denote the maximum force and heat load amplitude values.

3. Solution of Soil Control Equation

Dimensionless processing was carried out for values in Equations (1)-(3), which is expressed by

$$\begin{aligned} r^* &= V\eta r, \\ u_r^{S*} &= V\eta u_r^S, \\ t^* &= V^2\eta t, \\ \tau_0^* &= V^2\eta\tau, \\ \theta^{S*} &= \frac{\beta_1\theta^S}{\lambda^S + 2G^S}, \\ M^* &= \frac{\beta_1 M}{\lambda^S + 2G^S}, \\ \sigma_{ij}^{S*} &= \frac{\sigma_{ij}^S}{\lambda^S + 2G^S}, \\ P^* &= \frac{P}{\beta_2}, \\ V &= \sqrt{\frac{\lambda^S + 2G^S}{\rho^S}}, \\ \eta &= \frac{\rho^S c_s}{\kappa^S}. \end{aligned} \tag{9}$$

For convenient calculation, the asterisk is omitted. By substituting Equation (9) into Equation (1)-(3) and performing Laplace transform, the following expressions s can be obtained:

$$\frac{\partial \overline{e}^S}{\partial r} - \frac{\partial \overline{\theta}^S}{\partial r} - \frac{\partial \overline{M}}{\partial r} = s^2 \overline{u}_r^S \tag{10}$$

$$s\left(1 + \tau_0 s\right)\left(\overline{\theta}^S + \varepsilon\overline{e}^S + \varepsilon\alpha_1\overline{M}\right) = \nabla^2\overline{\theta}^S \tag{11}$$

$$\nabla^2\overline{e}^S + \alpha_1\nabla^2\overline{\theta}^S + \alpha_2 s\left(1 + \tau s\right)\overline{M} = \alpha_3\nabla^2\overline{M} \tag{12}$$

where

$$\alpha_1 = \frac{c_1 \rho^S V^2}{\beta_1 \beta_2},$$
$$\alpha_2 = \frac{\rho^S V^2}{\beta_2^2 D\eta},$$
$$\alpha_3 = \frac{b\rho^S V^2}{\beta_2^2}, \tag{13}$$
$$\varepsilon = \frac{T_0 \beta_1^2}{\left(\rho^S\right)^2 c_s V^2}$$

By combining Equations (10)-(12), we can obtain the following:

$$\left(\nabla^6 - \xi_1 \nabla^4 + \xi_2 \nabla^2 - \xi_3\right)\left(\overline{e}^S, \overline{\theta}^S, \overline{M}\right) = 0 \tag{14}$$

where

$$\begin{aligned}
x_1 &= s\left(1 + \tau_0 s\right), \\
x_2 &= s\left(1 + \tau_0 s\right)\varepsilon, \\
x_3 &= s\left(1 + \tau_0 s\right)\varepsilon\alpha_1, \\
x_4 &= s\left(1 + \tau s\right)\alpha_2, \\
\xi_1 &= \frac{1}{x_3\left(\alpha_3 - 1\right)}\left[\left(x_3 + \alpha_3 x_2\right)\left(x_3 - x_1\right) - x_2 x_4\right. \\
&\quad \left. + \left(x_3 + x_2\right)\left(\alpha_3 x_1 + x_4 + x_3\alpha_3\right) + s^2 x_3 \alpha_3\right] \\
\xi_2 &= \frac{1}{x_3\left(\alpha_3 - 1\right)}\left[x_2 x_4\left(x_3 - x_1\right) + \left(x_2 + x_3\right)x_1 x_4\right. \\
&\quad \left. + x_3 s^2\left(\alpha_3 x_1 + x_4 + x_3\alpha_1\right)\right] \\
\xi_3 &= \frac{1}{x_3\left(\alpha_3 - 1\right)} x_1 x_3 x_4 s^2
\end{aligned} \tag{15}$$

According to Helmholtz decomposition theory, (14) can be further decomposed to form

$$\left(\nabla^2 - k_1^2\right)\left(\nabla^2 - k_2^2\right)\left(\nabla^2 - k_3^2\right)\left(\overline{e}^S, \overline{\theta}^S, \overline{M}\right) = 0 \tag{16}$$

where

$$\begin{aligned}
k_1^2 &= \frac{1}{3}\left(2p\sin q + \xi_1\right), \\
k_2^2 &= \frac{1}{3}\left[\xi_1 - p\left(\sqrt{3}\cos q + \sin q\right)\right], \\
k_3^2 &= \frac{1}{3}\left[\xi_1 + p\left(\sqrt{3}\cos q - \sin q\right)\right], \\
p &= \sqrt{\xi_1^2 - 3\xi_2},\ q = \frac{1}{3} ar\sin\left(-\frac{2\xi_1^3 - 9\xi_1\xi_2 + 27\xi_3}{2p^3}\right)
\end{aligned} \tag{17}$$

Based on the properties of Bessel function and the variables at infinity when the boundary conditions are zero, the volumetric strain, temperature gradient, and diffusion flow intensity can be obtained as follows:

$$\begin{aligned}
\overline{e}^S &= \sum_{i=1}^{3} K_0\left(k_i r\right) A_i \\
\overline{\theta}^S &= \sum_{i=1}^{3} K_0\left(k_i r\right) B_i \\
\overline{M} &= \sum_{i=1}^{3} K_0\left(k_i r\right) M_i
\end{aligned} \tag{18}$$

where A_i, B_i, M_i $(i = 1, 2, 3)$ are the undetermined coefficients.

Thus, the following expression for radial displacement can be obtained:

$$\overline{u}_r^S = -\sum_{i=1}^{3} \frac{A_i}{k_i} K_1\left(k_i r\right) \tag{19}$$

The Laplace transform was conducted on (4)-(6), and the (18) and (19) are substituted into it. Then, the expressions of radial stress, hoop stress, and chemical potential can be obtained as follows:

$$\overline{\sigma}_r^S = \sum_{i=1}^{3}\left[\frac{\beta^2}{r k_i} K_1\left(k_i r\right) A_i + \left(A_i - B_i - M_i\right) K_0\left(k_i r\right)\right] \tag{20}$$

$$\begin{aligned}
\overline{\sigma}_\theta^S = \sum_{i=1}^{3}\left\{\left[\left(1 - \beta^2\right) A_i - B_i - M_i\right] K_0\left(k_i r\right)\right. \\
\left. - \frac{\beta^2}{r k_i} K_1\left(k_i r\right) A_i\right\}
\end{aligned} \tag{21}$$

$$\overline{P} = \sum_{i=1}^{3}\left(-A_i - \alpha_1 B_i + \alpha_3 M_i\right) K_0\left(k_i r\right) \tag{22}$$

where $\beta^2 = 2G^S/(\lambda^S + 2G^S)$.

Because A_i, B_i, M_i $(i = 1, 2, 3)$ are linear independent constants, (18) and (19) can be substituted into (10) and (11), and the following expression is obtained:

$$\begin{aligned}
\chi_i &= \frac{k_i^2}{s\left(1 + \tau_0 s\right)} \\
A_i &= \frac{k_i^2\left(\varepsilon\alpha_1 + \chi_i - 1\right)}{\varepsilon\alpha_1\left(k_i^2 - s^2\right) + \varepsilon k_i^2} B_i \\
M_i &= \frac{\left(\chi_i - 1\right)\left(k_i^2 - s^2\right) - k_i^2\varepsilon}{\varepsilon\alpha_1\left(k_i^2 - s^2\right) + \varepsilon k_i^2} B_i
\end{aligned} \tag{23}$$

4. Lining Control Equation and Its Solution

The lining is regarded as a homogeneous elastic medium. Under these axisymmetric conditions, according to the classical thermoelastic theory, the motion equation and heat conduction equation are expressed as

$$\left(\lambda^{\mathrm{L}} + 2\mu^{\mathrm{L}}\right)\frac{\partial e^{\mathrm{L}}}{\partial r} - \beta^{\mathrm{L}}\frac{\partial \theta^{\mathrm{L}}}{\partial r} = \rho^{\mathrm{L}}\frac{\partial^2 u_r^{\mathrm{L}}}{\partial t^2} \tag{24}$$

$$\kappa^{\mathrm{L}}\nabla^2\theta^{\mathrm{L}} = \rho^{\mathrm{L}}c_{\mathrm{L}}\frac{\partial \theta^{\mathrm{L}}}{\partial t} + T_0\beta^{\mathrm{L}}\frac{\partial e^{\mathrm{L}}}{\partial t} \tag{25}$$

where $\lambda^{\mathrm{L}} = 2\nu^{\mathrm{L}}\mu^{\mathrm{L}}/(1-2\nu^{\mathrm{L}})$ and $\mu^{\mathrm{L}} = G^{\mathrm{L}}$ denotes the Lame constants, ν^{L} denotes the Poisson's ratio of the lining, G^{L} denotes the shear modulus, $e^{\mathrm{L}} = \partial(ru_r^{\mathrm{L}})/r\partial r$ denotes the volumetric strain, and u_r^{L} denotes the radial displacement of the lining. The grouping $\beta^{\mathrm{L}} = (3\lambda^{\mathrm{L}} + 2\mu^{\mathrm{L}})\alpha^{\mathrm{L}}$ denotes the linear heat expansion coefficient and ρ^{L} denotes the density of lining.

The heat and force coupling constitutive relationship in consideration of temperature effects is

$$\begin{aligned}\sigma_r^{\mathrm{L}} &= 2\mu^{\mathrm{L}}\frac{\partial u_r^{\mathrm{L}}}{\partial r} + \lambda^{\mathrm{L}}e^{\mathrm{L}} - \beta^{\mathrm{L}}\theta^{\mathrm{L}}\\ \sigma_\theta^{\mathrm{L}} &= 2\mu^{\mathrm{L}}\frac{u_r^{\mathrm{L}}}{r} + \lambda^{\mathrm{L}}e^{\mathrm{L}} - \beta^{\mathrm{L}}\theta^{\mathrm{L}}\end{aligned} \tag{26}$$

To solve (24) and (25), the following dimensionless values are introduced:

$$\begin{aligned}\theta^{\mathrm{L}*} &= \frac{\beta_1\theta^{\mathrm{L}}}{\lambda^{\mathrm{S}} + 2G^{\mathrm{S}}},\\ u_r^{\mathrm{L}*} &= V\eta u_r^{\mathrm{L}},\\ \sigma_{ij}^{\mathrm{L}*} &= \frac{\sigma_{ij}^{\mathrm{L}}}{\lambda^{\mathrm{S}} + 2G^{\mathrm{S}}}\end{aligned} \tag{27}$$

After the Laplace transform was performed on Equations (24) and (25), they can be manipulated to form

$$\frac{\partial \overline{e}^{\mathrm{L}}}{\partial r} - m_1\frac{\partial \overline{\theta}^{\mathrm{L}}}{\partial r} = s^2 m_2 \overline{u}_r^{\mathrm{L}} \tag{28}$$

$$\nabla^2\overline{\theta}^{\mathrm{L}} = sn_1\overline{\theta}^{\mathrm{L}} + sn_2\overline{e}^{\mathrm{L}} \tag{29}$$

where

$$\begin{aligned}n_1 &= \frac{\rho^{\mathrm{L}}c_{\mathrm{L}}}{\eta\kappa^{\mathrm{L}}},\\ n_2 &= \frac{\beta^{\mathrm{L}}T_0}{\beta_1\eta\kappa^{\mathrm{L}}\left(\lambda^{\mathrm{S}} + 2G^{\mathrm{S}}\right)},\\ m_1 &= \frac{\beta^{\mathrm{L}}\left(\lambda^{\mathrm{S}} + 2G^{\mathrm{S}}\right)}{\beta_1\left(\lambda^{\mathrm{S}} + 2G^{\mathrm{S}}\right)},\\ m_2 &= \frac{\rho^{\mathrm{L}}V^2}{\left(\lambda^{\mathrm{L}} + 2G^{\mathrm{L}}\right)}.\end{aligned} \tag{30}$$

Equations (23) and (24) are combined and the expression for volumetric strain and temperature gradient can be expressed according to the solution method of (16):

$$\overline{e}^{\mathrm{L}} = \sum_{i=1}^{2}\left(K_0\left(\delta_i r\right)D_i + I_0\left(\delta_i r\right)E_i\right) \tag{31}$$

$$\overline{\theta}^{\mathrm{L}} = \sum_{i=1}^{2}\left(K_0\left(\delta_i r\right)G_i + I_0\left(\delta_i r\right)H_i\right) \tag{32}$$

where $\delta_{1,2}^2 = (d_1 \pm \sqrt{d_1^2 - 4d_2})/2$, $d_2 = s^2 n_1 s m_2$, $d_1 = s^2 m_2 + n_1 s + n_2 s m_1$, and D_i, E_i, G_i, H_i are undetermined coefficients.

Using the basic properties of the Bessel function, the radial displacement of the lining can be obtained from Equation (31):

$$\overline{u}_r^{\mathrm{L}} = -\sum_{i=1}^{2}\left[\frac{K_1\left(\delta_i r\right)}{\delta_i}D_i - \frac{I_1\left(\delta_i r\right)}{\delta_i}E_i\right] \tag{33}$$

Since D_i, E_i, G_i, H_i are linear independent constants, (31) and (32) are substituted into (28), and the following expressions can be obtained:

$$\begin{aligned}G_i &= \frac{\delta_i^2 - s^2 m_2}{\delta_i^2 m_1}D_i\\ H_i &= \frac{\delta_i^2 - s^2 m_2}{\delta_i^2 m_1}E_i\end{aligned} \tag{34}$$

The Laplace transform is used on Equation (26). By substituting Equations (31)-(33) into the s-domain expressions, the radial and hoop stresses of the tunnel lining are expressed as follows:

$$\begin{aligned}\overline{\sigma}_r^{\mathrm{L}} = &\sum_{i=1}^{2}\left[\left(n_3 - \frac{\beta^{\mathrm{L}}}{\beta_1}\frac{\delta_i^2 - s^2 m_2}{m_1\delta_i^2}\right)K_0\left(\delta_i r\right)\right.\\ &\left. + n_4\frac{K_1\left(\delta_i r\right)}{r\delta_i}\right]D_i\\ &+ \sum_{i=1}^{2}\left[\left(n_3 - \frac{\beta^{\mathrm{L}}}{\beta_1}\frac{\delta_i^2 - s^2 m_2}{m_1\delta_i^2}\right)I_0\left(\delta_i r\right) - n_4\frac{I_1\left(\delta_i r\right)}{r\delta_i}\right]\\ &\cdot E_i\end{aligned} \tag{35}$$

$$\begin{aligned}\overline{\sigma}_\theta^{\mathrm{L}} = &\sum_{i=1}^{2}\left[\left(n_6 - \frac{\beta^{\mathrm{L}}}{\beta_1}\frac{\delta_i^2 - s^2 m_2}{m_1\delta_i^2}\right)K_0\left(\delta_i r\right)\right.\\ &\left. - n_4\frac{K_1\left(\delta_i r\right)}{r\delta_i}\right]D_i\\ &+ \sum_{i=1}^{2}\left[\left(n_6 - \frac{\beta^{\mathrm{L}}}{\beta_1}\frac{\delta_i^2 - s^2 m_2}{m_1\delta_i^2}\right)I_0\left(\delta_i r\right) + n_4\frac{I_1\left(\delta_i r\right)}{r\delta_i}\right]\\ &\cdot E_i\end{aligned} \tag{36}$$

where

$$n_3 = \frac{\lambda^{\mathrm{L}} + 2G^{\mathrm{L}}}{\lambda^{\mathrm{S}} + 2G^{\mathrm{S}}},$$
$$n_4 = \frac{2G^{\mathrm{L}}}{\lambda^{\mathrm{S}} + 2G^{\mathrm{S}}}, \quad (37)$$
$$n_6 = \frac{\lambda^{\mathrm{L}}}{\lambda^{\mathrm{S}} + 2G^{\mathrm{S}}}$$

5. Boundary Conditions

Assuming that the lining outer diameter is entirely in close contact with the soil and there is no relative slip, the continuity condition is satisfied at the interface, there is no reflection of the elastic wave, and the contact thermal resistance is ignored. It is assumed that the chemical potential of the lining and soil contact surface is zero. A continuous model is employed to simulate the tunnel and soil. For the surface contact between the lining and soil ($r = R_2$), the following can be obtained:

$$\overline{u}_r^{\mathrm{S}} = \overline{u}_r^{\mathrm{L}},$$
$$\overline{\sigma}_r^{\mathrm{S}} = \overline{\sigma}_r^{\mathrm{L}},$$
$$\overline{\theta}^{\mathrm{S}} = \overline{\theta}^{\mathrm{L}}, \quad (38)$$
$$\overline{\sigma}_\theta^{\mathrm{S}} = \overline{\sigma}_\theta^{\mathrm{L}},$$
$$\overline{P} = 0$$

Since the explosion load is equivalent to the combination of temperature and force load, for the inner boundary of the lining ($r = R_1$), there is

$$\overline{\sigma}_r^{\mathrm{L}} = \overline{q}(s), \quad (39)$$
$$\overline{\theta}^{\mathrm{L}} = \overline{\theta}(s)$$

By substituting (18)-(22), (32), (33), (35), and (36) into (38) and (39), a set of seven expressions with seven unknowns can be found. Therefore, the solution of the thermoelastic dynamic response for the deep-buried circular tunnel lining-soil system under explosion load can be obtained by solving these equations.

6. Theoretical Degenerate Solution to the Problem

6.1. Solution without considering the Diffusion Effect. When $\beta_2 = 0, c_1 = 0, b = 0$, the model can be simplified into a thermoelastic dynamic response of the system without considering the diffusion effect. At this time, the model degenerates into a generalized thermoelastic model, and the equation of motion (1) of the soil can be written as

$$\left(\lambda^{\mathrm{S}} + 2\mu^{\mathrm{S}}\right)\frac{\partial e^{\mathrm{S}}}{\partial r} - \beta_1\frac{\partial \theta^{\mathrm{S}}}{\partial r} = \rho^{\mathrm{S}}\frac{\partial^2 u_r^{\mathrm{S}}}{\partial t^2} \quad (40)$$

The heat conduction Equation (2) can be written as

$$\left(\frac{\partial}{\partial t} + \tau_0\frac{\partial^2}{\partial t^2}\right)\left(\rho^{\mathrm{S}} c_{\mathrm{s}}\theta^{\mathrm{S}} + \beta_1 T_0 e^{\mathrm{S}}\right) = \kappa^{\mathrm{S}}\nabla^2\theta^{\mathrm{S}} \quad (41)$$

Their constitutive relationship is changed as follows:

$$\sigma_r^{\mathrm{S}} = 2\mu^{\mathrm{S}}\frac{\partial u_r^{\mathrm{S}}}{\partial r} + \lambda^{\mathrm{S}} e^{\mathrm{S}} - \beta_1\theta^{\mathrm{S}} \quad (42)$$

$$\sigma_\theta^{\mathrm{S}} = 2\mu^{\mathrm{S}}\frac{u_r^{\mathrm{S}}}{r} + \lambda^{\mathrm{S}} e^{\mathrm{S}} - \beta_1\theta^{\mathrm{S}} \quad (43)$$

6.2. Solution of the Problem without Lining. When the thickness of the lining is zero, that is, $h = 0$, the material parameters of the lining are equal to the material parameters of the soil, and it can be simplified to a cylindrical hole without a lining. At this time, the boundary condition at $r = R_2$ should be

$$\overline{\sigma}_r^{\mathrm{S}} = -\overline{q}(s),$$
$$\overline{\theta}^{\mathrm{S}} = \overline{\theta}(s), \quad (44)$$
$$\overline{P} = 0$$

By substituting Equations (20)-(22) into (44)

$$\sum_{i=1}^{3}\left[\frac{\beta^2}{R_2 k_i}K_1(k_i R_2)A_i + (A_i - B_i - M_i)K_0(k_i R_2)\right] = -\overline{q}(s) \quad (45)$$

$$\sum_{i=1}^{3}K_0(k_i r)B_i = \overline{\theta}(s) \quad (46)$$

$$\sum_{i=1}^{3}(-A_i - \alpha_1 B_i + \alpha_3 M_i)K_0(k_i r) = 0 \quad (47)$$

Therefore, the expression for the undetermined coefficient B_i can be obtained, getting the thermoelastic response of the infinite elastic body around the cylindrical cavity under load from the explosion.

6.3. The Comparison of Results with Existing Literature. In [20], the thermoelastic coupling dynamic response of an infinite elastic body around a circular tunnel under a step thermal shock load was explored. The thickness of the lining is zero and the parameters of the lining are equal to those of the soil. The following boundary conditions are satisfied, which can be simplified to the solution seen in [20]:

$$\overline{\sigma}_r^{\mathrm{S}} = 0,$$
$$\overline{\theta}^{\mathrm{S}} = \overline{\theta}(s), \quad (48)$$
$$\overline{P} = 0$$

where $\overline{\theta}(s) = ((1 - e^{-s})/s^2)\theta_0$.

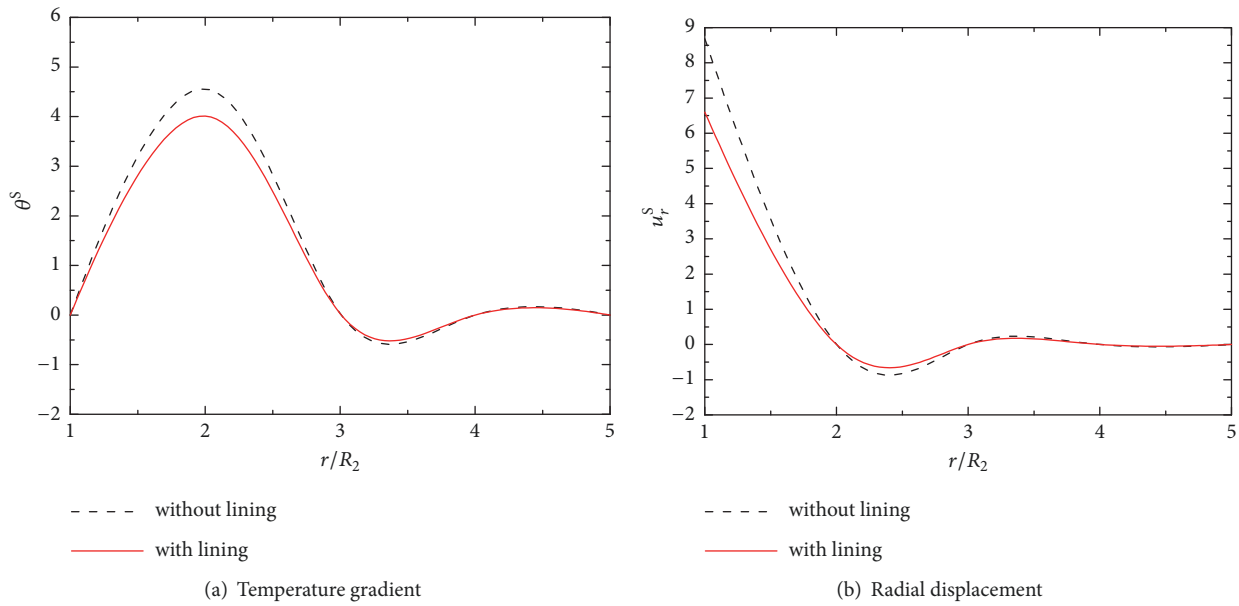

(a) Temperature gradient (b) Radial displacement

Figure 3: Comparison of calculation results with or without lining.

7. Numerical Analysis and Numerical Results

It is difficult to directly perform Laplace inverse transformation on expressions such as (35) and (36). In this paper, numerical methods are used to perform inverse Laplace transforms to develop closed-form results for the temperature gradient, radial displacement, stress, and chemical potential distribution of lining and soil system under explosion load. The following Crump numerical inversion method is used [33].

If we let the function $F(s)$ be the Laplace transform of the function $F(t)$, then the Crump inversion algorithm of Laplace inverse transform is

$$F(t) \approx \frac{e^{at}}{T^*}\left\{\frac{1}{2}F(a) + \sum_{k=1}^{\infty}\left[\begin{array}{c}\mathrm{Re}\left[F\left(a+\frac{k\pi i}{T^*}\right)\right]\cos\frac{k\pi t}{T^*} \\ -\mathrm{Im}\left[F\left(a+\frac{k\pi i}{T^*}\right)\right]\sin\frac{k\pi t}{T^*}\end{array}\right]\right\} \tag{49}$$

If $|F(t)| < Me^{\alpha t}$, the error is $|\varsigma| \le Me^{\upsilon}e^{-2T^*(a-\upsilon)}$, where, $T^* > t/2$.

The parameters of the soil in case study refer to [20], and the specific parameters are as follows: $G^S = 3.86\times10^7$Pa, $\nu^S = 0.3$, $\rho^S = 1800\mathrm{kg/m}^3$, $\tau_0 = 0.02$s, $\tau = 0.2$s, $D = 0.85\times10^{-8}$, $T_0 = 293$K, $\alpha_t = 1.78\times10^{-5\circ}\mathrm{C}^{-1}$, $\alpha_c = 1.2\times10^{-4\circ}\mathrm{C}^{-1}$, $c_s = 2000\mathrm{m}^2\mathrm{s}^{-2\circ}\mathrm{C}^{-1}$, $\kappa^S = 3.8$W, $c_1 = 12$, $b = 9\times10^5$, $\bar{t} = 1$.

The parameters of the lining are as follows: $\rho^L = 2440\mathrm{kg/m}^3$, $G^L = 3.5\times10^8$Pa, $\nu^L = 0.55$, $h = 0.2$m, $R_1 = 3$m, $R_2 = 3.2$m, $\alpha^L = 4.78\times10^{-5}\mathrm{K}^{-1}$, $\kappa^L = 5.6$W, $c_L = 2710\mathrm{m}^2\cdot\mathrm{s}^{-2\circ}\mathrm{C}^{-1}$.

7.1. Comparative Analysis

7.1.1. The Comparison of Calculated Results without Lining. As shown in Figure 3, the calculated results for the temperature gradients and radial displacements with and without a lining are analyzed with respect to the change of the radius of the tunnel. According to the abovementioned parameters, the dimensionless time is $t = 0.5$. It can be seen that the thickness of the lining has a great deal of influence on the temperature gradient and temperature within the lining. For the peak value, the temperature gradient values without the lining are obviously larger than those seen with the lining. With increased radius, the influence of the lining on the temperature gradient decreases gradually. This is because the thermal conduction of the lining material is considered in the explosion, and the physical parameters such as the heat transfer coefficient and the linear thermal expansion coefficient of the lining are substantially different from those of soil. When considering the influence of lining, the radial displacement of the soil is smaller than it is without the lining. This is due to the lining having greater rigidity than the soil.

7.1.2. Comparison of Calculation Results with Results from Existing Literature. Figure 4 shows that the dimensionless time is $t = 0.5$, and the solution (A) of this paper is simplified to compare it to the solution described in [20], and, compared with the calculated result (B) of [20], the temperature gradients and radial displacements of the soil are found to be consistent, which verifies the correctness and accuracy of the calculated results.

7.2. Parameter Analysis

7.2.1. Time-Domain Analysis Procedure. Figure 5 shows set plots of the variation of the temperature gradient in the soil

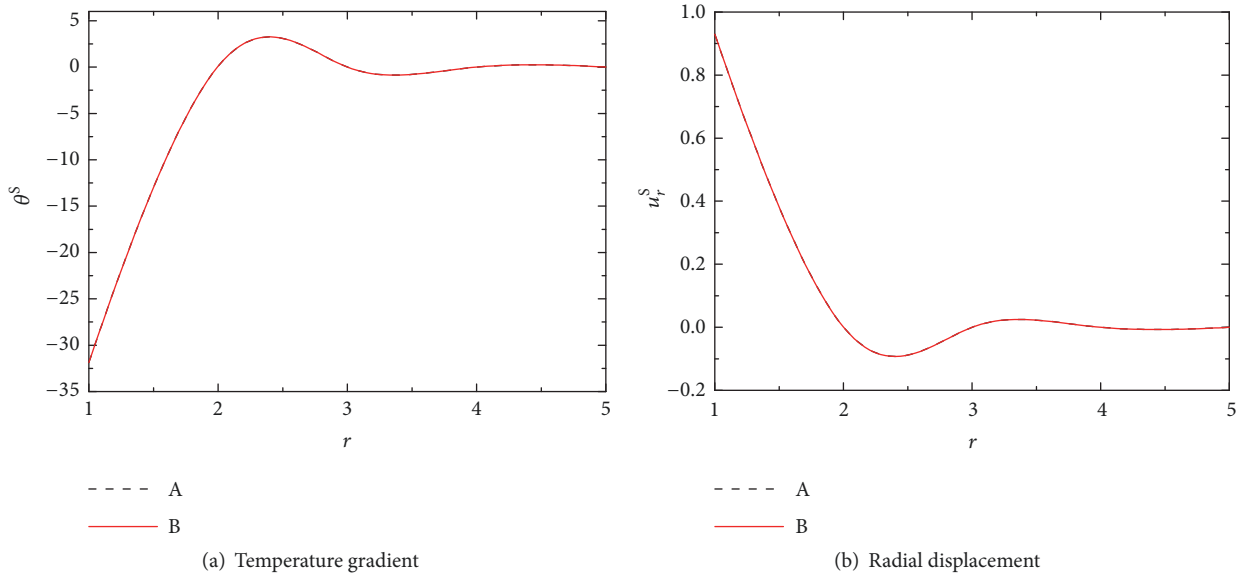

(a) Temperature gradient (b) Radial displacement

Figure 4: Comparison of calculated results with results from [20].

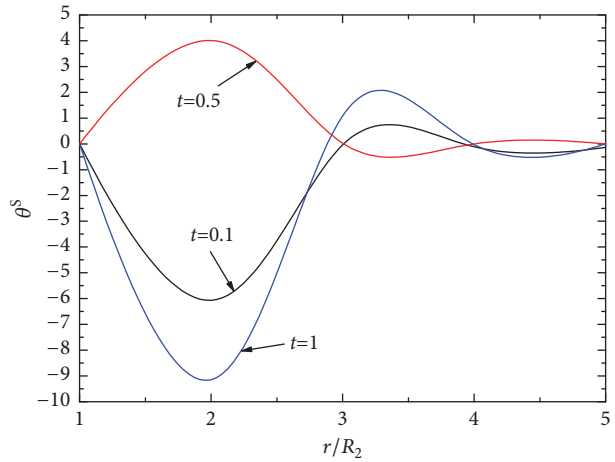

Figure 5: Variations of the temperature gradient with respect to the radius at different times.

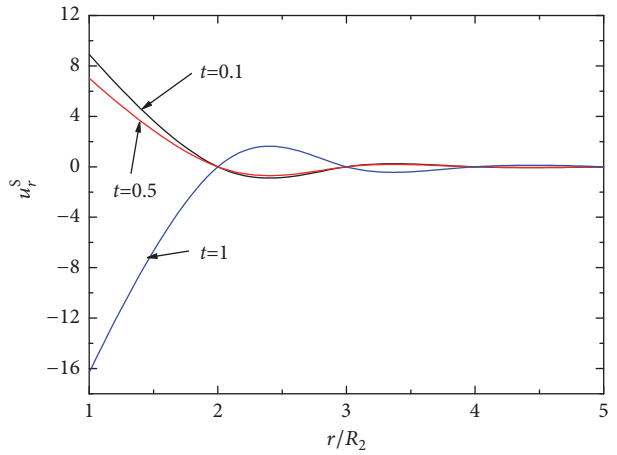

Figure 6: Curves showing variation of the radial displacement with radius at different times.

with respect to the radius, when the dimensionless time is $t = 0.1$, $t = 0.5$, and $t = 1$. It can be seen that, under the action of the explosion, the temperature gradient fluctuates, and the heat wave propagates at a finite speed, and multiple reflections occur after the force source reaches the inner wall of the lining. For $t = 0.5$ and $r/R_2 < 2.8$, the peak value of the temperature gradient has a positive value. As the radius increases, the temperature gradient gradually decreases and finally approaches zero. The peak magnitude is negative for $t = 0.1$ and $t = 1$. As the radius increases, a positive peak value appears first and then gradually decreases. This is caused by the interaction and mutual influence of temperature, stress, and chemical field under the explosive load, that is, the coupling effect of heat, force, and chemical.

Figure 6 shows the attenuation rule for radial displacement of the soil with radii, at $t = 0.1$, $t = 0.5$, and $t = 1$. It can be seen that, at the interface between the lining and the soil under the action of the explosion load, the radial displacement of the soil reaches its maximum positive value at $t = 0.1$ and $t = 0.5$, and the radial displacement at the time $t = 0.1$ is greater than the displacement at $t = 0.5$. As the radius increases, the displacement amplitude gradually decreases. At time $t = 1$, the radial displacement of the soil reaches its maximum magnitude at a negative value. As the radius increases, the displacement shows a positive peak value first and then gradually decreases. This is because the explosion wave is emitted from the center, and multiple reflections will occur after encountering the inner wall of the lining. The maximum pressure is caused by the tendency of oscillating attenuation.

Figure 7 shows a set of curves for the variation of the radial stress of the soil with radius at the time $t = 0.1$, $t = 0.5$,

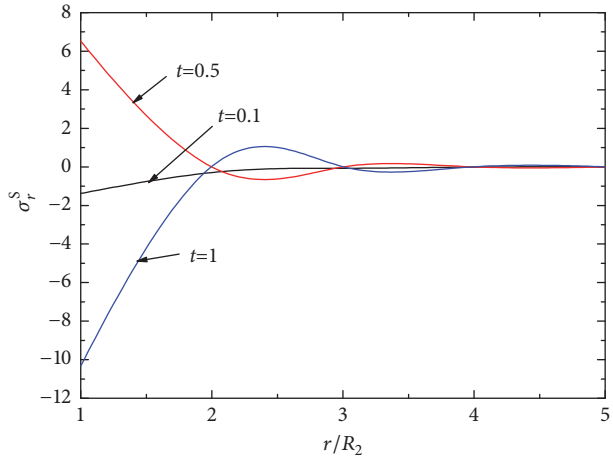

FIGURE 7: Curves showing variation of the radial stress with respect to radius at different times.

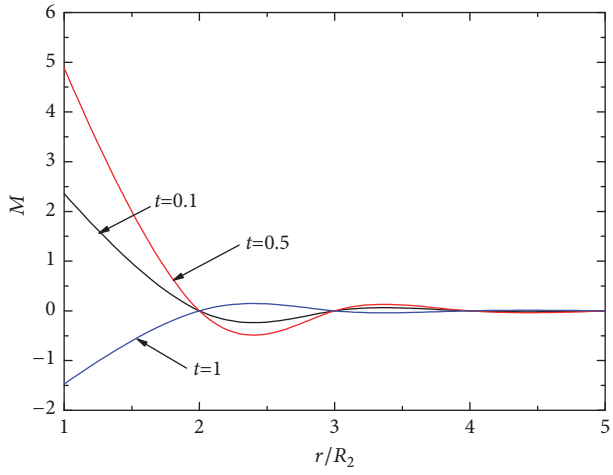

FIGURE 8: Curve showing variation of the diffusion flow intensity with respect to radius at different times.

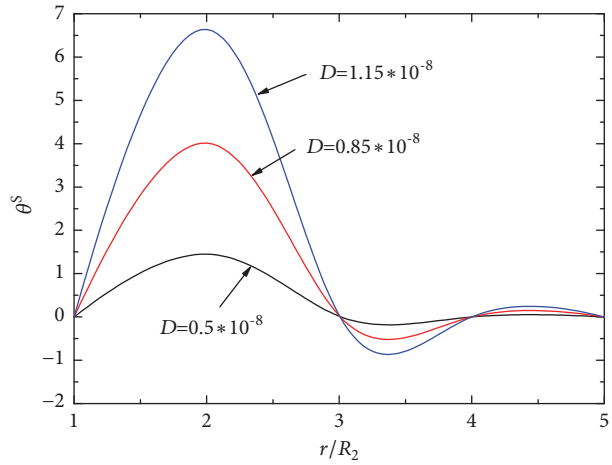

FIGURE 9: Curves showing the influence of the diffusion coefficient on the temperature gradient.

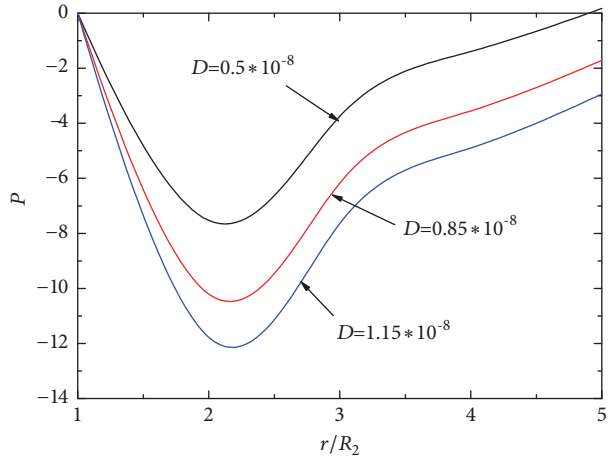

FIGURE 10: Curves showing the influence of the diffusion coefficient on the chemical potential.

and $t = 1$. It can be seen that, at $t = 0.5$, the radial stress at the interface between the lining and the soil is positive, while, at the time $t = 0.1$ and $t = 1$, the stress has a negative value at the interface between the lining and the soil. This is due to the lining being subjected to shock waves and high temperatures and pressures during the explosion.

Figure 8 shows a curve for variation of the diffusion flow intensity with respect to radius at times $t = 0.1$, $t = 0.5$, and $t = 1$. In the process of heat transfer, there is an interinfiltration between substances, that is, a thermal diffusion effect. It can be seen that, under the action of explosive load, like heat conduction, heat diffusion propagates at a finite speed. At the time $t = 0.5$, the diffusion flow intensity at the interface between the lining and the soil reaches its maximum magnitude at a positive value, and the value at $t = 0.1$ is larger than that at $t = 1$. As the radius increases, a negative value occurs first and then gradually decreases. At the time $t = 1$, the diffusion flow intensity at the interface between the lining and the soil reaches its maximum value at a negative value and gradually decreases with increasing radius.

7.2.2. The Impact of the Diffusion Coefficient. Figures 9 and 10 show the effect of the diffusion coefficient on the temperature gradient and chemical potential. When these are evaluated at time $t = 0.5$, the relevant coefficients are $D = 0.5 \times 10^{-8}$, $D = 0.85 \times 10^{-8}$, and $D = 1.15 \times 10^{-8}$. It can be seen that the thermal diffusion effects of the coupled temperature field, material diffusion, and strain field are more obvious in the elastic medium, and the diffusion coefficient has a great deal of effect on the peak value of the temperature gradient. As the diffusion coefficient increases, the peak value increases significantly, especially within the radius range $1 < r/R_2 < 3$. The diffusion coefficient has also a great deal of influence on the chemical potential of the soil. As the diffusion coefficient increases, the negative peak value of the chemical potential gradually increases. As the radius increases, the chemical potential gradually decreases.

8. Conclusions

The effect of thermal diffusion is considered in this paper based on the generalized thermal diffusion theory and the classical thermal elasticity theory. An analytical solution is used to study the thermoelastic dynamic response of a deeply buried circular tunnel lining-soil system under a sudden load from an explosion within the tunnel's cavity. The thermoelastic dynamic response of a soil-lining system under the explosion's load is solved using the Laplace transform and the Helmholtz decomposition techniques. By using continuity boundary conditions, the corresponding numerical solution is obtained via inverse Laplace transformation. The effects of lining and soil parameters on the thermoelastic dynamic response of the system are analyzed, and the conclusions can be summarized as follows.

(1) Due to the large difference in physical parameters such as heat transfer coefficient and linear thermal expansion coefficient between the lining and the soil, the lining thickness has a significant impact on the temperature gradient and displacement. At the peak value of the temperature gradient, the temperature gradient without the lining is significantly larger than that with lining, and the radial displacement of the soil is smaller than the calculated result for the case without the lining.

(2) At different times, such as $t = 0.1$, $t = 0.5$ and $t = 1$, the rules for the changes in the temperature gradient, displacement, stress, and diffusion flow intensity with radius are significantly different. As the radius increases, these values gradually decrease.

(3) The diffusion coefficient has a significant effect on the peak values of the temperature gradients and chemical potential. As the diffusion coefficient increases, the peak value increases significantly within the range $1 < r/R_2 < 3$, and the negative peak value of the chemical potential gradually increases. As the radius increases, the chemical potential value gradually decreases.

(4) This study shows the propagation of heat and diffusion concentration at finite speed, rather than the infinite speed propagation under the action of explosive load.

Data Availability

All data used to support the findings of this study were supplied by the Natural Sciences Foundation Committee of China under Grant no. 41472254. Requests for access to these data should be made to the corresponding author Jinming Xu at Department of Civil Engineering, Shanghai University, Shanghai, 200072, China, xjming@shu.edu.cn. Phone number is +86 13166143882 and fax number is +86 021 56382059.

Conflicts of Interest

The authors declare that they have no conflicts of interest.

Acknowledgments

Financial supports for the study were provided by the Natural Sciences Foundation Committee of China under Grant no. 41472254, the National Special Projects for International Science and Technology Cooperation of China under Grant no. 2014DFE90040, the Zhejiang Provincial Natural Science Foundation of China under Grant no. LGF18E080010, and the Zhejiang Key R&D Program of China under Grant no. 2019C03120. These supports are gratefully acknowledged.

References

[1] Y.-Q. Cai, C.-Z. Chen, and H.-L. Sun, "Transient dynamic response of tunnels subjected to blast loads in saturated soil," *Chinese Journal of Geotechnical Engineering*, vol. 33, no. 3, pp. 361–367, 2011.

[2] M. Gao, J. Y. Zhang, Q. S. Chen, G. Y. Gao, J. Yang, and D. Y. Li, "An exact solution for three-dimensional (3D) dynamic response of a cylindrical lined tunnel in saturated soil to an internal blast load," *Soil Dynamics and Earthquake Engineering*, vol. 90, pp. 32–37, 2016.

[3] Y. Wang and G.-Y. Gao, "Analysis of transient dynamic response of cylindrical lined cavity in nearly saturated soil," *Rock and Soil Mechanics*, vol. 36, no. 12, pp. 3400–3409, 2015.

[4] M.-Y. Liu and Z.-F. Lu, "Analysis of dynamic response of Yangtze River tunnel subjected to contact explosion loading," *Journal of Wuhan University of Technology*, vol. 29, no. 1, pp. 113–117, 2007.

[5] U. Zakout and N. Akkas, "Transient response of a cylindrical cavity with and without a bonded shell in an infinite elastic medium," *International Journal of Engineering Science*, vol. 35, no. 13-12, pp. 1203–1220, 1997.

[6] W. Nowacki, "Dynamic problems of thermodiffusion in elastic solids," *Progress in Color, Colorants and Coatings*, vol. 15, no. 2, pp. 105–128, 1974.

[7] W. Nowacki, "Dynamic problems of diffusion in solids," *Engineering Fracture Mechanics*, vol. 8, no. 1, pp. 261–266, 1976.

[8] M. Dryja, "Difference and finite-element methods for the dynamical problem of thermodiffusion in an elastic solid," *Archives of Mechanics*, vol. 29, no. 1, pp. 81–96, 1977.

[9] R. Kumar and V. Chawla, "Effect of rotation on surface wave propagation in a elastic layer lying over a thermodiffusive elastic half-space having imperfect boundary," *Mechanics of Advanced Materials and Structures*, vol. 18, no. 5, pp. 352–363, 2011.

[10] H. W. Lord and Y. Shulman, "A generalized dynamical theory of thermoelasticity," *Journal of the Mechanics and Physics of Solids*, vol. 15, no. 5, pp. 299–309, 1967.

[11] A. E. Green and K. A. Lindsay, "Thermoelasticity," *Journal of Elasticity*, vol. 2, no. 1, pp. 1–7, 1972.

[12] A. E. Green and P. M. Naghdi, "Thermoelasticity without energy dissipation," *Journal of Elasticity*, vol. 31, no. 3, pp. 189–208, 1993.

[13] W. T. Zhao, J. H. Wu, Y. Bai, and Z. H. Han, "Generalized thermoelastic analysis for a solid sphere under thermal shock," *Journal of Xi'an Jiaotong University*, vol. 47, no. 7, pp. 108–113, 2013.

[14] X. Wang and X. Xu, "Thermoelastic wave induced by pulsed laser heating," *Applied Physics A: Materials Science & Processing*, vol. 73, no. 1, pp. 107–114, 2001.

[15] D. S. Chandrasekharaiah, "One-dimensional wave propagation in the linear theory of thermoelasticity without energy dissipation," *Journal of Thermal Stresses*, vol. 19, no. 8, pp. 695–710, 1996.

[16] R. S. Dhaliwal and H. H. Sherief, "Generalized thermoelasticity for anisotropic media," *Quarterly of Applied Mathematics*, vol. 38, no. 1, pp. 1–8, 1980.

[17] H. H. Sherief and H. A. Saleh, "A problem for an infinite thermoelastic body with a spherical cavity," *International Journal of Engineering Science*, vol. 36, no. 4, pp. 473–487, 1998.

[18] B. Singh, "Reflection of P and SV waves from free surface of an elastic solid with generalized thermodiffusion," *Journal of Earth System Science*, vol. 114, no. 2, pp. 159–168, 2005.

[19] M. Aouadi, "A problem for an infinite elastic body with a spherical cavity in the theory of generalized thermoelastic diffusion," *International Journal of Solids and Structures*, vol. 44, no. 17, pp. 5711–5722, 2007.

[20] R.-Y. Zheng, G.-B. Liu, and G.-J. Tang, "Thermodynamic response of a cylindrical tunnel in the theory of generalized thermoelastic diffusion," *Journal of National University of Defense Technology*, vol. 30, no. 3, pp. 27–31, 2008.

[21] G.-b. Liu, H.-l. Yao, Y. Yang et al., "Coupling thermo-hydro-mechanical dynamic response of a porous elastic mdium," *Rock and Soil Mechanics*, vol. 28, no. 9, pp. 1784–1788, 2007.

[22] Z. Lu, H.-L. Yao, G.-B. Liu, and X.-W. Luo, "Dynamic response of coupling thermo-hydro-mechanical foundation subjected to harmonic line loads," *Rock and Soil Mechanics*, vol. 31, no. 7, pp. 2309–2316, 2010.

[23] H. H. Sherief, A. M. A. El-Sayed, and A. M. Abd El-Latief, "Fractional order theory of thermoelasticity," *International Journal of Solids and Structures*, vol. 47, no. 2, pp. 269–275, 2010.

[24] H. Sherief and A. M. Abd El-Latief, "Effect of variable thermal conductivity on a half-space under the fractional order theory of thermoelasticity," *International Journal of Mechanical Sciences*, vol. 74, no. 13, pp. 185–189, 2013.

[25] H. M. Youssef, "Theory of fractional order generalized thermoelasticity," *Journal of Heat Transfer*, vol. 132, no. 6, pp. 1–7, 2010.

[26] M. A. Ezzat, A. S. El-Karamany, and A. A. El-Bary, "On thermo-viscoelasticity with variable thermal conductivity and fractional-order heat transfer," *International Journal of Thermophysics*, vol. 36, no. 7, pp. 1–14, 2015.

[27] M. Ezzat and S. Ezzat, "Fractional thermoelasticity applications for porous asphaltic materials," *Petroleum Science*, vol. 13, no. 3, pp. 168–178, 2016.

[28] Y.-s. Xu, Z.-d. Xu, T.-h. He et al., "Analysis on fractional-order generalized thermoelastic problem for ideal adhesion sandwich plate under thermal shock," *Journal of Southeast University (Natural Science Edition)*, vol. 47, no. 1, pp. 130–136, 2017.

[29] E. A. Barzilovich, A. E. Verstakov, V. A. Nikulin, N. V. Sirotinkin, and V. A. Sytov, "The influence of the fractional composition of a filler on thermal conductivity of a polymer composition," *Polymer Science - Series D*, vol. 7, no. 1, pp. 57–60, 2014.

[30] J. Bourret, N. Tessier-Doyen, B. Naït-Ali et al., "Effect of the pore volume fraction on the thermal conductivity and mechanical properties of kaolin-based foams," *Journal of the European Ceramic Society*, vol. 33, no. 9, pp. 1487–1495, 2013.

[31] I. A. Abbas, "Eigenvalue approach on fractional order theory of thermoelastic diffusion problem for an infinite elastic medium with a spherical cavity," *Applied Mathematical Modelling: Simulation and Computation for Engineering and Environmental Systems*, vol. 39, no. 20, pp. 6196–6206, 2015.

[32] Y.-z. Cao and Z.-s. Lu, "Numerical simulations of blast flow fields in closed blast-resistant containers," *Chinese Journal of High Pressure Physics*, vol. 15, no. 2, pp. 127–132, 1997.

[33] K. S. Crump, "Numerical inversion of Laplace transforms using a Fourier series approximation," *Journal of the ACM*, vol. 23, no. 1, pp. 89–96, 1976.